International Journal of Modern Trends in Engineering and Research
www.ijmter.com
e-ISSN No.:2349-9745, Date: 2-4 July, 2015

Design and Development of Push Pull DC-DC Converter by ZCS/ZVS to Electrical Vehicle (EVs) Applications

Veeresh H [1], Dr. Ashok Kusagur [2]

[1]*Research Scholar, VTU RRC, EEE Dept., A.M.G.O.I, veeresh.hv@gmail.com.*
[2]*EEE Dept. U.B.D.T. College of Engg.,ashok.kusagur@gmail.com.*

Abstract-Electrical Vehicle (EVs) is taking a leading role in upcoming research area of Renewable energy source applications. In this paper, a novel Push–Pull converter is proposed, which has simple and reduced gating signal used by the (in this proposed) converter due to two primary devices (switches S_1 and S_2) with common ground to supply. Fixed frequency duty cycle modulation (100k Hz) with source voltage (12V) is used to design proposed converter to regulate the out-put. This topology yields high efficiency through low circulating currents, zero current switching (ZCS) and low-current switching of the primary side devices, ZVS of the secondary side switches, and in the majority of switching cycle direct power transfer to the load. An active-clamped circuit is also used to reduce the voltage spike on the power switches for raising the system reliability. The designed converter has been simulated using Simulink Model (Matlab-Software) tools. Simulation results for input voltage V_{in} = 12 V, output voltage V_o = 300 V, output power P_o = 250W, device switching frequency f_s = 100 kHz are verified through the output waveforms which shows better performance of the system.

Keywords-Current-fed converter, Push-Pull DC-DC converter, soft-switching, ZCS/ZVS, EVs, Active-clamped, Matlab-Software

I. INTRODUCTION

Electrical Vehicle (EVs) is taking a leading role in upcoming research area of renewable energy source applications. Transportation electrification has received significant interest owing to limited supply of fossil fuels and concern of global climate change [1-3]. Battery based Electric vehicles (EVs) and Fuel Cell Vehicles (FCVs) are emerging as viable solutions for transportation electrification with lower emission, better vehicle performance and higher fuel economy. Compared with pure battery based EVs, FCVs are quite appealing with the merits of zero-emission, satisfied driving range, short refueling time, high efficiency, and high reliability.

A diagram of a typical FCV propulsion system is shown in Fig. 1 [4-6]. A DC - DC converters are widely used in regulated switch - mode dc power supplies and in dc motor drive applications. Often the input to the converters is an unregulated dc voltage, which is obtained by rectifying the line voltage, and therefore it will fluctuate due to changes in the line voltage magnitude. Switch mode dc - dc converters are used to convert the unregulated dc input into a controlled dc output at a desired voltage level. Converters are very often used with an electrical isolation transformer in the switch - mode dc power supplies and almost always without an isolation transformer in case of dc motor drives. DC/DC converters are utilized to develop high voltage bus for the inverter.

The energy storage system (ESS) is used to overcome the limitations of lacking energy storage capability and fast power transient of FCVs. Bidirectional converter with high boost ratio and high

efficiency is required to connect the low-voltage ESS and high voltage dc link bus[7-20]. This can significantly reduce conduction loss of primary side switches. However, voltage-fed converters suffer from several limitations, i.e. high pulsating current at input, limited soft-switching range, rectifier diode ringing, duty cycle loss (if inductive output filter), high circulating current through devices and magnetic, and relatively low efficiency for high voltage amplification and high input current applications. Compared with voltage-fed converters, current-fed converters exhibit smaller input current ripple, lower diode voltage rating, lower transformer turns-ratio, negligible diode ringing, no duty cycle loss, and easier current control ability. Besides, current-fed converters can precisely control the charging and discharging current of ESS, which helps achieving higher charging/discharging efficiency. Thus current-fed converter is more feasible for the application of ESS in FCVs.

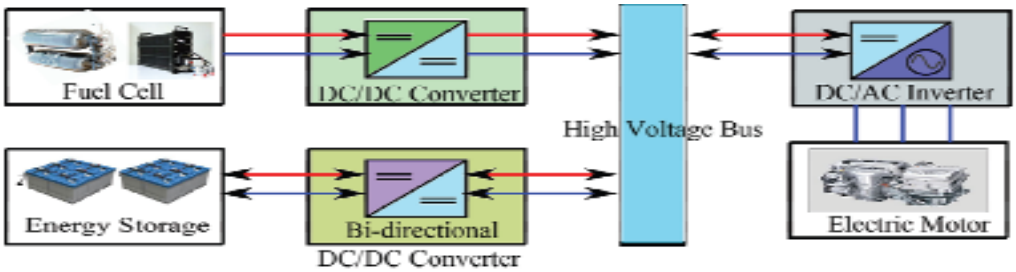

Figure 1. Diagram of a FCV propulsion system

The leakage inductance and parasitic capacitance of the HF transformer were utilized to achieve zero current switching (ZCS) in [18-20]. However, resonant current is much higher than input current that increases the current stress of devices and magnetics requiring higher VA rating components. In this paper, a push-pull converter is proposed as shown in Fig. 2.

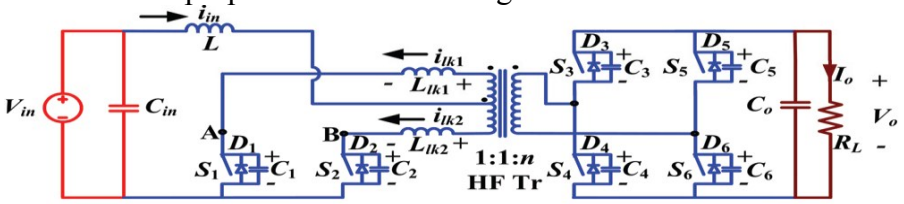

Figure 2. Proposed push-pull DC/DC converter

DC/DC converters are widely used in regulated switch - mode dc power supplies and in dc motor drive applications. Often the input to the converters is an unregulated dc voltage, which is obtained by rectifiring the line voltage, and therefore it will fluctuate due to changes in the line voltage magnitude. Switch mode dc - dc converters are used to convert the unregulated dc input into a controlled dc output at a desired voltage level. Converters are very often used with an electrical isolation transformer in the switch - mode dc power supplies and almost always without an isolation transformer in case of dc motor drives.

Switching frequency in the megahertz range , even tens of megahertz, are being contempt to reduce the size and the weight of transformers and filter components and, hence, to reduce the cost as well as the size and the weight of power electronics converters. Realistically, the switching frequencies can be increased to such high values if the problems of switch stresses, switching losses, and the EMI associated with the switch-mode converters can be overcome. The output in some of these circuits is controlled by controlling the operating frequency; in others a constant frequency square wave or PWM control can be used with some additional constraints to provide ZVS/ZCS. ZCS topology where the switch turns on and turns off at zero current. The peak resonant current flows through the switch but the peak switch voltage remains the same as in its switch mode counter parts.

ZVS topology where the switch turns on and turns off at zero voltage. The peak resonant voltage appears across the switch but the peak switch current remains the same as in its switch mode counterparts.

In this paper is to design a push pull converter, which can gain output 300V DC from 12V DC input. This work also try to implement MATLAB tools simulation of push pull converter with a center tap high frequency transformer. The objectives are realized and outlined in various Sections as follows: Steady-state operation of the converter is explained and its mathematical analysis, detailed converter design procedure is illustrated in Section II. Analysis and design are verified by simulation results using MATLAB in Section III. Simulation results of 300V are demonstrated to validate and show the converter performance in Section IV.

II. DESIGN AND OPERATION OF CONVERTER

2.1 Design of Converter

In this Section, converter design procedure is illustrated by a design example for the following specifications: input voltage V_{in} = 12 V, output voltage V_o = 150 to 300V, output power Po=250W and switching frequency f_s = 100 kHz. The design equations are presented to determine the components' ratings. It helps selection of the components as well as to predict the converter performance theoretically.

(1) Maximum voltage across the primary switches is

$$V_{p,sw} = \frac{2 \cdot V_o}{n} \qquad 2.1$$

(2) Voltage conversion ratio or input and output voltages are related as

$$V_o = \frac{n \cdot V_{in}}{2 \cdot (1-d)} \qquad 2.2$$

Where d is the duty cycle of primary switches. This equation is derived on the condition that anti-parallel diode conduction time (e.g. interval 6) is quite short and negligible with the intention to ensure ZCS of primary switches without significantly increasing the peak current. However, at light load condition of converter, (fuel cell stack is supplying most of the power to propulsion system and battery is supplying only auxiliary load), and the anti-parallel diode conduction time is comparatively large, (2.1) is not valid any more. Due to the existence of longer anti-parallel diode conduction period, the output voltage is boosted to higher value than that of nominal boost converter.

(3) Average input current is $I_{in} = P_o/(\eta V_{in})$. Assuming an ideal efficiency η of 95%, I_{in} = 21.9 A.

(4) The selection of transformer turns-ratio is selected to maintain duty cycle d >0.5. By using (2.1),

$$n < \frac{2 \cdot V_{o,\min} (1 - d_{\min})}{V_{in}} \qquad 2.3$$

Therefore, maximum value of n = 12.5 for $V_{o,min}$=150V. Fig. 3 shows variation of total value of series inductances L_{lk_T}(H) with respect to power transferring ability P (W) for four values of turns-ratio. With the increase of turns-ratio, the value of L_{lk_T}decreases. It is difficult to realize low leakage inductance with high turns-ratio. In addition, higher turns-ratio may lead to more transformer loss because of higher copper loss, higher eddy current from proximity effect and higher core loss due to larger size. However, increasing the turns-ratio can reduce the maximum voltage across the primary switches, which permits use of low voltage devices with low on-state resistance. Thus conduction losses in the primary side semiconductor devices can be significantly reduced. An optimum turns-ratio n =10, duty ratio d = 0.8 are selected to achieve an acceptable trade-off. Output voltage can be

regulated from 150 V to 300 V by modulating the duty ratio from 0.6 to 0.8 including battery voltage variation due to its charging and discharging characteristics.
(5) Leakage inductance L_{lk_T}= 22.2 µH for the given values. Here, series inductors L_{lk1} and L_{lk2} are chosen to be equal to L_{lk1}= L_{lk2}=3.4 µH.
Unequal design of series inductors L_{lk1} and L_{lk2} is also permitted.
Where V_{in}=12V, V_o=300V, n=10, P_o=250W, f_s=100kHz, I_{in}=21.93A, $T_{DR}/T_s=(n.V_{in})/V_o$=0.2 duty cycle=0.85 for ZVS and 0.8 for proposed ZCS topology. The efficiency of the proposed converter is higher due to reduced losses associated with clamp circuit and main primary switches.

2.2 Operation of Converter

For the sake of simplicity, the following assumptions are made to study the operation and explain the analysis of the converter:
a) Boost inductor L is large enough to maintain constant current through it.
b) All the components are ideal.
c) Series inductors L_{lk1} and L_{lk2} include the leakage inductances of the transformer. The total value of L_{lk1} and L_{lk2} is represented as L_{lkT}. L_{lk} represents the equivalent series inductor reflected to the high voltage side.
d) Magnetizing inductance of the transformer is infinitely large.

Interval 1 (t_o<t<t_1): In this interval, primary side switch S_2 and anti-parallel body diode D_3 and D_6 of the secondary side H bridge switch are conducting. Power is transferred to the load through HF transformer. The non-conducting secondary device S_4 and S_5 are blocking output voltage V_{DC} and the non-conducting primary device S_1 is blocking reflected output voltage $2V_o/n$. The values of current through various components are: i_{S1}=0, i_{S2}=I_{in} ,i_{Llk1}=0, i_{Llk2}= I_{in}, $i_{D3,6}$ = I_{in}/n. Voltage across the switch S_1: V_{S1}=$2V_o/n$. Voltage across the switch $S_{4,5}$: $V_{S4,5}$= V_o.

Interval 2 (t_1<t<t_2): At t=t_1, primary switch S_1 is turned-on. The corresponding snubber capacitor C_1 discharges in a very short period of time. At the end of this interval, S_1 is fully conducting and C_1 is completely discharged.

Interval 3 (t_2<t<t_3): Now all two primary switches are conducting. Reflected output voltage appears across series inductors L_{lk1} and L_{lk2}, diverting/transferring the current through switch S_2 to S_1. It causes current through previously conducting device S_2 to reduce linearly. It also results in conduction of switch S_1 with zero current which helps reducing associated turn-on loss. Thecurrents through various components are given by.

$$i_{Llk1} = i_{s1} = \frac{2V_o}{nL_{lk\_T}}.(t - t_2) \quad 2.4$$

$$i_{Llk2} = i_{s2} = I_{in} - \frac{2V_o}{nL_{lk\_T}}.(t - t_2) \quad 2.5$$

$$i_{D3} = \frac{I_{in}}{n} - \frac{2V_{DC}}{n^2 L_{lk\_T}}.(t - t_2) \quad 2.6$$

Where L_{lk_T}= L_{lk1}+L_{lk2}. Before the end of this interval t=t_3, the body diode D_3 is conducting. Therefore S_3 can be gated on for ZVS turn -on. At the end of this interval, D_3 commutates naturally. Current through all primary devices reaches $I_{in}/2$.Final values are: i_{Llk1}= i_{Llk2}=$I_{in}/2$, i_{S1}= i_{S2}=$I_{in}/2$, $i_{D3,6}$=0.

Interval 4 (t_3<t<t_4): In this interval, secondary device$S_3$is turned-on with ZVS. Currents through all the switching devices continue increasing or decreasing with the same slope as interval 3. At the end of this interval, the primary device S_2 commutates naturally with ZCC and the respective current i_{S2} reaches zero obtaining ZCS. The full current, i.e. input current is taken over by other device S_1. Final values are: i_{Llk1}=i_{S1}=I_{in}, i_{Llk2}=i_{S2} =0, $i_{S3,6}$ = I_{in}/n.

Interval 5 (t_4<t<t_5): In this interval, the leakage inductance current i_{Llk1} increases further with the same slope and anti- parallel body diode D_2 starts conducting causing extended zero voltage to

appear across commutated switch S_2 to ensure ZCS turn- off. Now, the secondary device $S_{3,6}$ are turned-off. At the end of this interval, current through switch S_1 reaches its peak value. This interval should be very short to limit the peak current though the transformer and switch reducing the current stress and kVA ratings. The currents through operating components are given by

$$i_{S1} = i_{Llk1} = I_{in} + \frac{2V_o}{nL_{lk\_T}}.(t - t_4) \quad 2.7$$

$$i_{D2} = -i_{Llk2} = \frac{2V_o}{nL_{lk\_T}}.(t - t_4) \quad 2.8$$

$$i_{S3,6} = \frac{I_{in}}{n} + \frac{4V_o}{n^2 L_{lk\_T}}.(t - t_4) \quad 2.9$$

Interval 6 (t_5<t<t_6): During this interval, secondary switch S_3 is turned-off. Anti-parallel body diode of switch S_4 takes over the current immediately. Therefore, the voltage across the transformer primary reverses polarity. The current through the switch S_1 and body diodes D_2 also start decreasing. The currents through operating components are given by

$$i_{S1} = i_{Llk1} = I_{sw,peak} - \frac{V_O}{nL_{lk\_T}}.(t - t_5) \quad 2.10$$

$$i_{D2} = -i_{Llk2} = I_{D2,peak} - \frac{V_O}{nL_{lk_T}}.(t - t_5) \quad 2.11$$

$$i_{D4,5} = \frac{I_{lk,peak}}{n} - \frac{4V_o}{n^2 L_{lk\_T}}.(t - t_5) \quad 2.12$$

At the end of this interval, current through D_2 reduce to zero and is commutated naturally. Current through S_1 reaches I_{in}. Final values: $i_{Llk1} = i_{S1} = I_{in}$, $i_{Llk2} = i_{D2} = 0$, $i_{D4} = I_{in}/n$.

Interval 7 (t_6<t<t_7): In this interval, snubber capacitor C_2 charges to V_{DC}/n in a short period of time. Switch $S_2$is in forward blocking mode now.

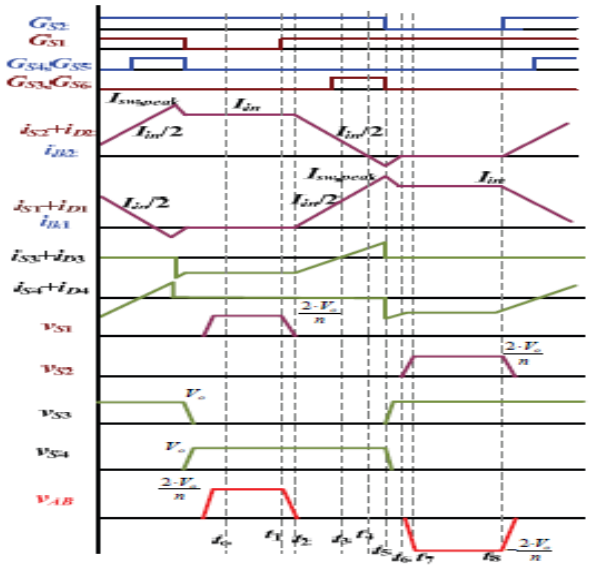

Figure 3. Operating waveforms of proposed ZCS current-fed converter

Interval 8 (t_7<t<t_8): In this interval, currents through$S_1$and transformer are constant at input current I_{in}. Current through anti-parallel body diode of the secondary switch D_4isatI_{in}/n. The final values are: $i_{Llk1} = i_{S1} = I_{in}$, $i_{Llk2} = i_{S2} = 0$, $i_{D4} = I_{in}/n$. Voltage across the switch S_2 $V_{S2} = V_o/n$. In this half HF cycle, current has transferred from switch S_2 to S_1, and the transformer current has reversed its polarity.

III. RESULTS AND DISCUSSION

Proposed converter has been simulated using software MATLAB. Simulation results for input voltage V_{in} = 12 V, output voltage V_{out} = 300 V, output power P_o = 250W, device switching frequency f_s = 100 kHz are illustrated in Fig. 4. Simulation results coincide closely with theoretically predicted waveforms. It verifies the steady-state operation and analysis of the converter presented in Section II. Waveforms of current through the input inductor L and voltage V_{sec} are shown in Fig. 4. The ripple frequency of input inductor current i_L is 2x $f_s$resulting in a reduction in size. Voltage waveform V_{sec} shows that voltage across the primary switches is naturally clamped at low voltage i.e. $2V_o/n$.

Fig. 4 shows current waveforms through primary switches S_1 and S_2 and secondary switches S_3 and S_4 including the currents flowing through their respective body diodes, phase shifted with each other by 180^o (S_1vs S_2, S_5vs S_6). Primary switch currents ($I_{(S1)}$, $I_{(S2)}$) are diverted from one switch (say S_1) to the other one (S_2) causing one switch to rise to I_{in} and the other one to fall to zero.

This clearly demonstrates claimed ZCC of primary switches. The negative primary currents correspond to conduction of body diodes before the switches are turned-off, which ensures ZCS turn-off of the primary switches. As shown in current waveforms of S_3 and S_4 in Fig. 4, the anti-parallel diodes of switches conduct prior to the conduction of corresponding switches, which verifies ZVS of the secondary side switches.

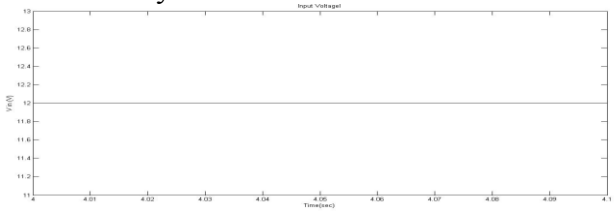

(a) Time v/s input voltage

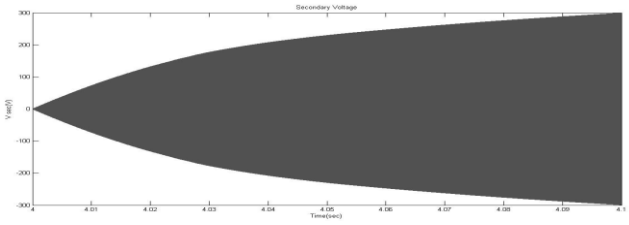

(b) Time v/s secondary voltage

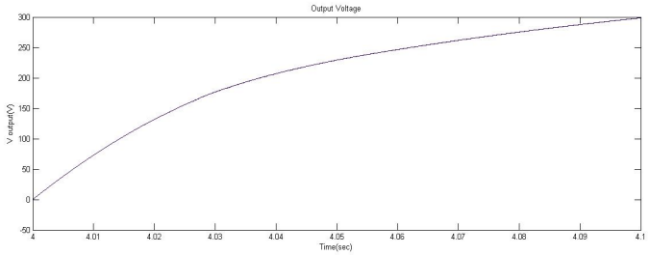

(c) Time v/s output voltage

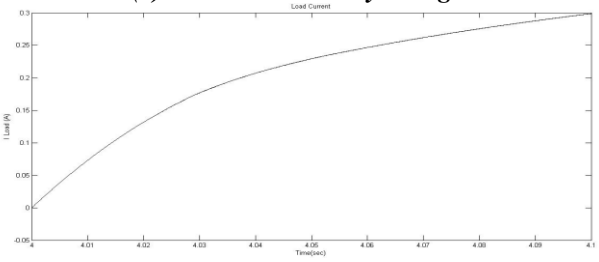

(d) Time v/s Load Current

Figure 4. Simulation results for out-put voltage 300V at input voltage 12V and Current through load i_L, voltage V_{sec}.

IV. CONCLUSION

This paper presents a ZCS/ZVS Push pull DC/DC Converter for application of the ESS in FCVs. A secondary side modulation method is proposed to eliminate the problem of voltage spike across the semiconductor devices at turn-off. ZCS of primary side devices and ZVS of secondary side devices are achieved, which reduces the switching losses significantly. Soft-switching is inherent and is maintained independent of load. Once soft-switching is designed to be obtained at rated power, it is guaranteed to happen at reduced load unlike voltage-fed converters. Turn-on switching transition loss of primary devices is also shown to be negligible. Hence maintaining soft-switching of all devices substantially reduces the switching loss and allows higher switching frequency operation for the converter to achieve a more compact and higher power density system.

Proposed secondary modulation achieves natural commutation of primary devices and clamps the voltage across them at low voltage (reflected output voltage) independent of duty cycle. Usage of low voltage devices results in low conduction losses in primary devices, which is significant due to higher currents on primary side.

The proposed modulation method is simple and easy to implement. These merits make the converter promising for interfacing low voltage dc bus with high voltage dc bus for higher current applications such as FCVs, front-end dc/dc power conversion for renewable (fuel cells/PV) inverters, UPS, micro grid, V2G, and energy storage. The specifications are taken for FCV but the proposed modulation, design, and the demonstrated results are suitable for any general application of current-fed converter (high step-up). Similar merits and performance will be achieved.

REFERENCES

[1] PanXuewei,Akshay K rathore, "naturally clamped zero current commuted soft-switching current –fed Push pull DC/DC converter:analysis, Design, Experimental Results", IEEE Trans.Power Electronics,0885-8993©2013.

[2] PanXuewei, Akshay K Rathore, "Current-fed Soft-Switching Push-pull Front-end Converter Based Bidirectional Inverter for Residential Photovoltaic Power System",10.1109/TPEL.2014.2301495, IEEE Transactions on Power Electronics.

[3] Akshay K. Rathore, Prasanna U R, "Analysis, Design, and Experimental Results of Novel Snubberless Bidirectional Naturally Clamped ZCS/ZVS Current-Fed Half-Bridge DC/DC Converter for Fuel Cell Vehicles" IEEE TRANSACTIONS ON INDUSTRIAL ELECTRONICS, VOL. 60, NO. 10, OCTOBER 2013.

[4] A. Khaligh and Z. Li, "Battery, ultracapacitor, fuel cell, and hybrid energy storage systems for electric, hybrid electric, fuel cell, and plug-in hybrid electric vehicles: State of the art", IEEE Trans. on Vehicular Technology, vol. 59, no. 6, pp. 2806- 2814, Oct. 2009.

[5] A. Emadi, and S. S. Williamson, "Fuel cell vehicles: opportunities and challenges," in Proc. IEEE PES, 2004, pp. 1640-1645.

[6] K. Rajashekhara, "Power conversion and control strategies for fuel cell vehicles," in Proc. IEEE IECON, 2003, pp. 2865-2870.

[7] A. Emadi, S. S. Williamson, and A. Khaligh, "Power electronics intensive solutions for advanced electric, hybrid electric, and fuel cell vehicular power systems," IEEE Trans. Power Electron., vol. 21, no. 3, pp. 567–577, May. 2006.

[8] T.-F. Wu, Y.-C.Chen, J.-G.Yang, and C.-L.Kuo, "Isolated bidirectional full-bridge DC–DC converter with a flyback snubber," IEEE Trans. Power Electron., vol. 25, no. 7, pp. 1915–1922, Jul. 2010.

[9] Y. Kim; I. Lee; I.Cho; G. Moon, "Hybrid dual full-bridge DC–DC converter with reduced circulating current, output filter, and conduction loss of rectifier stage for RF power generator application," IEEE Trans. Power Electron., vol.29, no.3, pp.1069-1081, March 2014

[10] Corradini, L.,Seltzer, D., Bloomquist, D., Zane, R., Maksimović, D., Jacobson, B., "Minimum Current Operation of Bidirectional Dual-BridgeSeries Resonant DC/DC Converters", IEEE Trans. Power Electron.,vol. 27, no.7, pp.3266-3276, July 2012.

[11] X. Li and A. K. S. Bhat, "Analysis and design of high-frequency isolated dual-bridge series resonant DC/DC converter," IEEE Trans. Power Electron., vol. 25, no. 4, pp. 850–862, Apr. 2010

[12] R.-J. Wai, C.-Y.Lin, and Y.-R. Chang, "High step-up bidirectional isolated converter with two input power sources," IEEE Trans. Ind. Electron., vol. 56, no. 7, pp. 2629–2643, Jul. 2009.

[13] Lizhi Zhu, "A Novel Soft-Commutating Isolated Boost Full-bridge ZVS-PWM DC-DC Converter for Bi-directional High Power Applications," IEEE Trans. Power Electron., vol. 21, no. 2, pp. 422–429, Mar. 2006.

[14] P. Xuewei and A. K. Rathore, "Novel Interleaved Bidirectional Snubberless Soft-switching Current-fed Full-bridge Voltage Doubler for Fuel Cell Vehicles," IEEE Transactions on Power Electronics, vol. 28, no. 12, Dec. 2013, pp. 5355-5546.

[15] A. K. Rathore and U. R. Prasanna, "Analysis, Design, and Experimental Results of Novel Snubberless Bidirectional Naturally Clamped ZCS/ZVS Current-fed Half-bridge Dc/Dc Converter for Fuel Cell Vehicles," IEEE Trans. Ind. Electron., no.99, Aug. 2012.

[16]S. J. Jang, C. Y. Won, B. K. Lee and J. Hur, "Fuel cell generation system with a new active clamping current-fed half-bridge converter," IEEE Trans. on Energy Conversion, vol. 22, no.2, pp. 332-340, June 2007.

[17] S. Han, H. Yoon, G. Moon, M. Youn, Y. Kim, and K. Lee, "A new active clamping zero-voltage switching PWM current-fed half bridge converter," IEEE Trans. Power Electron., vol.20, no.6, pp 1271-1279, Nov.2006.
[18]Tsai-Fu Wu, Jin-Chyuan Hung, Jeng-Tsuen Tsai, Cheng-Tao Tsai, and Yaow-Ming Chen, "An active-clamp push-pull converter for battery sourcing application," IEEE Trans. Industry Application., vol.44, no.1, pp.196-204, Jan.2008.
[19] C.L. Chu and C.H. Li, "Analysis and design of a current-fed zero-voltage-switching and zero-current-switching CL-resonant push-pull dc-dc converter," IET Power Electron., vol. 2, no. 4, pp. 456–465, Jul. 2009.
[20] Stanislaw Jalbrzykowski and TadeuszCitko, "Current-Fed Resonant Full-Bridge Boost DC/AC/DC Converter," IEEE Trans. Ind. Electron., vol. 55, no.3 ,pp.1198-1205, March 2008.

